Theoretical Guidelines of LPP-EUV Sources for HVM

Katsunobu Nishihara, Kazumi Fujima (a), Hiroyuki Furukawa (b), Takashi. Kagawa (c), Young Gwang Kang, Takako Kato (d), Fumihiro. Koike (e), Richard More (d), Masakatsu Murakami, Takashi Nishikawa (f), Akira Sasaki (g), Atsushi Sunahara (b),Hajime Tanuma (h), Vasilii Zhakhovskii, Shinsuke Fujioka, Hiroaki Nishimura, Yoshinori Shimada (b), Keiji Nagai, Takayoshi Norimatsu, Noriaki iyanaga,Yasukazu Izawa and Kunioki Mima

Institute of Laser Engineering, Osaka University, (a) Yamanashi University, (b) Institute for Laser Technology, (c) Nara Women's University, (d) National Institute for Fusion Science, (e) Kitazato University, (f) Okayama University, (g) JAEA-KANSAI, (h) Tokyo Metropolitan University,

Abstract

On the basis of our understanding, we here present theoretical guidelines of LPP-EUV sources for HVM to obtain higher EUV power, to reduce fast ion energy and their mitigation schemes. We propose to use CO_2 laser to obtain the high conversion efficiency (CE) of 4-6 %, and double laser pulses scheme to reduce the fast ion energy and to realize the minimum mass target. We discuss mainly physics related to our new guidelines.

I. Introduction

At the EUV source workshop in Vancouver, May 25, 2006, the joint EUV source power requirement was updated, i.e., the expression of source power was compromised from the view points of both resist performance and lifetime of consumables to 115 W@5mJ/cm2 – 180 W@10mJ/cm2 at IF. The increase of EUV power requires higher conversion efficiency (CE), more effective mitigation scheme of fast ions and debris. We have constructed both theoretical and experimental database, such as atomic data, dependence of CE on laser intensity, pulse duration and laser wavelength, energy spectra of charge separated fast ions for various laser and target conditions but mostly for tin targets. We have also proposed benchmarking of LPP-EUV source models at the workshop. On the basis of our understanding, we here present theoretical guidelines of LPP-EUV sources for HVM to obtain higher EUV power, to reduce fast ion energy and their mitigation schemes.

We have shown that the power balance model of CE [1] (see also Appendix A) predicts well many experimental results of CE [2]. On the basis of the power balance model, we will show that higher CE of 4 - 6 % can be obtained with the use of CO_2 (CO2) laser in Sec. II. We discuss advantage of double laser pulse scheme to realize the minimum mass target in Sec. III, and reduction of the fast ion energy, which may mainly cause damage of focusing mirror, with use of low initial density target in Sec. IV.

II. High Conversion Efficiency of 4-6 % by CO_2 Laser

Figure 1 shows the dependence of the maximum CE in (a) and optimum pulse duration in (b) on electron temperature and ion density with the laser intensity required to sustain expanding laser produced plasma obtained from the power balance model [1]. As shown in the figure very high CE of 4 – 6 % can be obtained in relatively low ion density region of 10^{17} – 10^{18} cm^{-3} and electron temperature of 30 – 50 eV. Low density requirement is due to opacity effect in tin plasma. Opacity of tin target with the electron temperature of 30 eV has been experimentally observed [3] and its absolute vale agrees with HULLAC calculation. Emissivity and absorption coefficient of 13.5 nm radiation are calculated by HULLAC code and shown in Fig. 2. Although the high emissivity is obtained in high density region, the absorption coefficient becomes very large in the high density region and most of EUV radiation can be absorbed in the expanding plasma. Therefore with use of 1.06 μm laser the maximum CE of 2 – 3 % is obtained with relatively short pulse duration of 2 – 3 ns [4], which agrees well with the power balance model prediction. Many experiments with longer pulse duration show the self-absorption dip in EUV spectra [4]. The optimum pulse duration can be about 10 ns or longer at low density region as shown in Fig. 2. In addition to the opacity effects, the spectral efficiency, the ratio of 13.5 nm emission with 2 % bandwidth to total emission, is large in the low density region as shown in Fig. 3, which also results in the higher CE in the low density region.

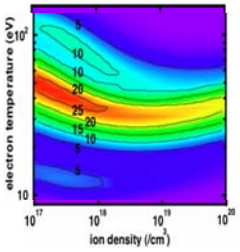

Fig. 3. Dependence of spectral efficiency (%), namely, the ratio of 13.5 nm emission with 2 % bandwidth to total radiation on electron temperature and ion density.

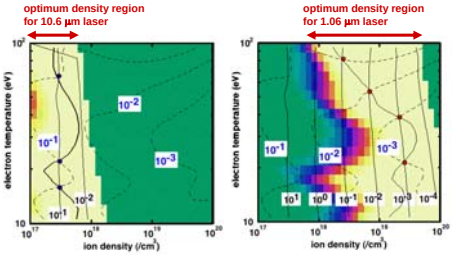

Fig.4. Dependence of absorption length (solid line: cm) of 10.6 μm laser in (a) and 1.06 μm laser (solid line: cm) in (b) and 13.5 nm radiation (dotted line: cm). Laser energy can be efficiently converted to 13.5 nm radiation in yellow region, where the laser absorption length becomes comparable to the absorption length of 13.5 nm radiation.

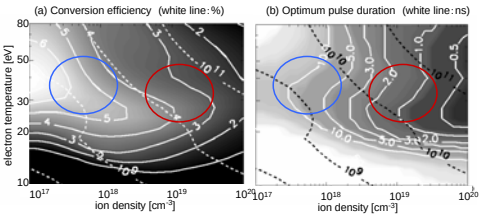

Fig. 1. Dependence of conversion efficiency (white line: %) in (a), required laser intensity (dotted line: W/cm^2) and optimum laser pulse duration (white line: ns) in (b) on electron temperature and ion density for Sn planar target. Red and blue circles indicate the parameter regions for 1.06 μm laser and 10.6 μm laser, respectively.

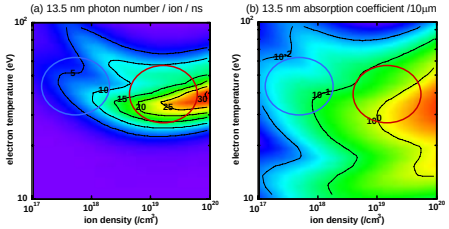

Fig. 2. Dependence of emissivity (photon number/ion/ns) (a) and absorption coefficient (/10 m) (b) of 13.5nm (2%BW) radiation on electron temperature and ion density. Red and blue circles indicate the parameter regions for 1.06 μm laser and 10.6 μm laser, respectively.

In order to realize the low density plasma, we have to choose proper laser wavelength and proper initial target density. High conversion from laser energy to 13.5 nm radiation energy can be obtained when the laser absorption length becomes comparable with the absorption length of 13.5 nm EUV radiation. Both absorption lengths are determined from the electron temperature and electron density as shown in Fig. 4. As shown in Fig. 4 the absorption length of 10.6 μm laser becomes comparable with that of 13.5 nm emission at ion density of 10^{17} – 10^{18} cm^{-3} (yellow region in Fig. 4). Those results predicts that the high CE of 4 – 6 % can be obtained with the use of CO2 laser.

III. Double Laser Pulse and Minimum Mass Target

As shown in Fig. A2, most of 13.5 nm radiation is emitted from the hot corona plasma, where ion density is less than 10^{19} cm^{-3} for 1.06 μm laser irradiation. Remaining high density region becomes only the source of neutral debris. Left figure in Fig. 5 shows experimental results of EUV CE and emission intensity from neutral Sn atoms as functions of Sn layer thickness coated on plastic plate and irradiated by 1.06 μm laser with intensity of 10^{11} W/cm^2[5]. CE does not change much for the thickness of 30 nm or more, while emission from neutral atoms increases exponentially with the increase of the tin layer thickness. Those results indicate there is a minimum mass required for

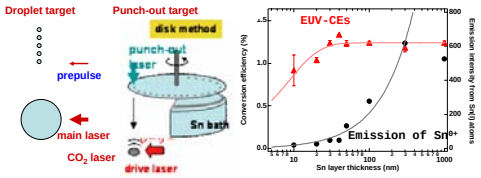

Fig. 5. Concept of LPP-EUV source for MVE with minimum mass target such as droplet target and punch-out target and with double laser pulses, prepulse with 1.06 μm laser and main pulse with10.6 μm laser. Right figure shows dependence of EUV-CE and emission from neutral Sn atom as functions of Sn layer thickness [5].

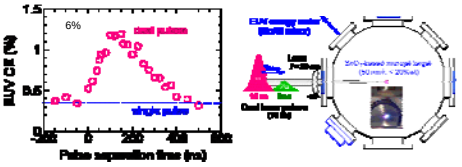

Fig. 6. Increase of EUV conversion efficiency observed in experiments with double laser pulses after Higashiguchi et al., [6]

LPP-EUV sources. The minimum mass is about a few tens micron meters in diameter with solid density. The minimum mass target can be realized with the use of droplet target and the punch-out target as shown in Fig. 5. In the punch-out target thin tin layer is coated on a plate transparent for 1.06 μm laser light. As discussed in Sec. II, the optimum ion density for EUV source is about 10^{17} – 10^{18} cm^{-3}. By irradiating pre-pulse or punch-out laser on the minimum mass targets the heated target expands and the optimum density of the source material can be obtained before the main CO2 laser. The increase of CE with the use of double laser pulses has been experimentally observed as shown in Fig. 6 after Higashiguchi et al. even for 1.06 μm laser [6].

The double laser pulse irradiation scheme can provide the optimum plasma density for LPP-EUV sources, but also it reduces fast ion energy. As will be discussed Sec. IV. fast ion energy is determined from electron temperature and initial plasma density. Fast ion energy spectroscopy measurements show that their energy becomes of the order of 10 keV for an initial solid target as shown in Fig. 7 [7]. It is till very difficult to mitigate those high energy ions. The double laser pulses scheme reduces the initial plasma density and thus the reduction of the fast ion energy is expected. This reduction also observed in experiments [6,7].

IV. Debris Mitigation

If the minimum mass target is realized, most dangerous debris can be fast ions. In order to mitigate fast ions by a magnetic field, its energy should be less than a few keV, since fast ions expand at least in a distance of two times of their gyro-radius as shown below. At energy of 10 keV, the gyro-radius becomes about 10 cm for magnetic field intensity of 1 T. We have developed an analytical model for fast ion energy [8] (see also Appendix B), which predicts well the experimental spectra of fast ion energy [8]. The model shows that the maximum fast ion energy is determined from the electron temperature and initial density as

$$\mathbf{E}_{max} \approx \frac{1}{2}\mathbf{m}_i\mathbf{v}_{max}^2 \approx 2\langle z\rangle \mathbf{T}_e \ln\left(\frac{\Lambda^2}{2}\ln\left(\frac{\Lambda^2}{2}\right)\right)$$

$$\Lambda^2 = \frac{\mathbf{R}_D^2}{\lambda_{De}^2} = \frac{e^2\mathbf{R}_D^2\langle z\rangle \mathbf{n}_0}{\varepsilon_0 \mathbf{T}_e} \propto \frac{\mathbf{n}_0^{1/3}}{\mathbf{T}_e} \qquad \mathbf{N} = \frac{4\pi}{3}\mathbf{R}_D^3\mathbf{n}_0 = \mathbf{const}$$

This formula indicates that the maximum energy decrease with the decrease of the initial density for a given initial total mass. The decrease of the maximum fast ion energy is also observed in the punch-out target [7] and the double laser pulses irradiation [6] as shown in Fig. 7. The maximum energy becomes less than1 keV for the punch-out target although it is 10 keV in solid density target.

The plasma expansion in a strong magnetic field has been studied with the use of a hybrid code, in which ion is treated as particles. As shown in Fig. 8, The ions expands to the distance of two times of their gyro-radius at half period of gyro-frequency and they mostly run away from the system along the magnetic field line without expanding much across the field. These results shows the fast ions with less than a few keV can be mitigated with the use of the magnetic field.

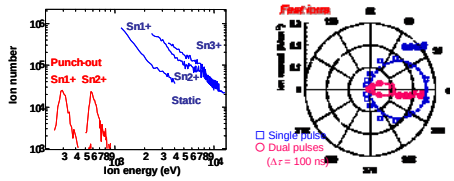

Fig. 7. Reduction of fast ion energy observed in punch-out target after S. Fujioka et al. [7] and droplet target with double pulses experiment after Higashiguchi et al. [6].

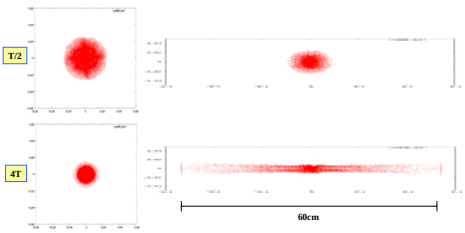

Fig. 8. Hybrid simulation of plasma expansion in a magnetic field at half cycle and 4th cycle of ion gyro-frequency.

V. Conclusion

We have proposed theoretical guidelines of LPP-EUV sources for HVM to obtain higher EUV power, to reduce fast ion energy and their mitigation schemes. We have shown that the use of CO_2 laser results in the high conversion efficiency of 4-6 %, with the optimum conditions for the laser intensity and pulse duration, which can be realized with present technology. It is also discussed that the double laser pulses scheme can reduce the fast ion energy and to realize the minimum mass target such as the droplet target and the punch-out target . We discuss physics related to our new guidelines on the bases of our theoretical models, which has been benchmarked with many experimental results.

Acknowledgments

A part of this work performed under the auspices of the Leading Project –promoted by MEXT, Japan. We also thank to Prof. H. Nakajima and Dr. Y. Kajishima at Kyushu University, they allow us to use their hybrid code for magnetic mitigation simulations.

Appendix A. Power Balance Model of Conversion Efficiency

Power balance model of CE has been developed [1]. Laser ablation plasma consists of two regions, high density cold region and low density hot region as shown in Fig. A1. Most of EUV radiation is emitted in the hot low density region, called as a corona plasma. Since the laser produced hot plasma expands into vacuum, no stationary plasma exists. Therefore energy balance consideration is not enough. Because of the high electron conductivity in the corona, we may assume that an isothermal expansion of the corona plasma follows the laser-ablation surface. The ion density and expansion velocity are given by following formula, which agrees well the results shown in Fig. A1.

$$n_i(x,t) = n_0 e^{-\frac{x}{c_s t}} \qquad v(x,t) = \frac{x}{t} + c_s$$

The energy fluxes required to sustain the isothermal expansion can be estimated from the sum of the kinetic expansion energy loss flux, ionization and internal energy loss flux and radiation energy flux. Their spatial profile are shown in Fig. A2. By knowing the density profile and expansion velocity we can estimated the loss fluxes as below. We have to taken the self absorption of the radiation into account in the plasma for the radiation loss flux. Atomic data such as emissivity, absorption coefficient and ionization state have been calculated with use of HULLAC code.

1. expansion kinetic energy loss flux

$$I_{kin} = \frac{d}{dt}\int_0^\infty \frac{1}{2}mv^2 n_i dx + \frac{1}{2}mc_s^2 n_0 c_s = 3Z^*(n_0,T_e)n_0 T_e c_s$$

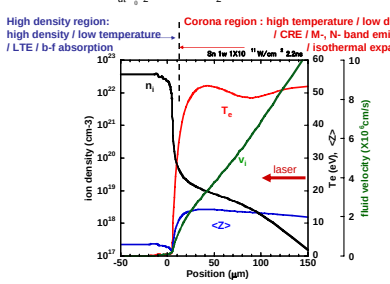

Fig. A1. Typical EUV source plasma profile, electron temperature (red line), ion density (black line), ion velocity (green line) and averag ionization state for planar Sn target irradiated with 1.06 μm laser with intensity of 10^{11} W/cm^2 with 2.2 ns FWHM (Full Width of Half Maximum).

2. ionization and internal energy loss flux

$$I_{ion} = \left[E_{ion}(n_0,T_e) + \frac{3}{2}Z^*(n_0,T_e)T_e\right]n_0 c_s$$

3. radiation energy flux

$$I_{rad} = \int_0^\infty\int_0^\infty j_\nu(n_i,T_e)\exp\left(-\int_x^\infty \kappa_\nu(n_i,T_e)dx'\right)dxd\nu$$

By assuming the sum of those loss flux balances with the absorbed laser flux, we can obtained the relation between the electron temperature and the laser intensity as shown Fig. A3. For Sn target the radiation loss dominates, approximately half of the laser flux. The CE from the incident laser to the EUV inband emission can the be estimated as

$$\eta_{EUV} = \frac{I_{EUV_CR} + I_{EUV_HD}}{I_{rad} + I_{ion} + I_{kin}}$$

$$I_{EUV_CR} = \frac{I_{rad_EUV}}{2} \qquad I_{EUV_HD} = I_{P,EUV}(T_R) \qquad 2\sigma T_R^4 = \frac{I_{rad}}{2}$$

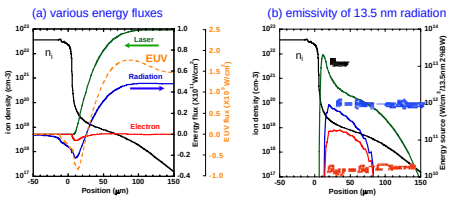

Fig. A2. Various energy fluxes in laser ablation plasma, laser flux (green), total radiation flux (blue), EUV 13.5 nm radiation with 2 % bandwidth (brawn) and electron heat flux (red) in (a), and emissivity of 13.5 nm radiation (green) with self absorption (blue) and 13.5 nm emission flux from surface in (b).

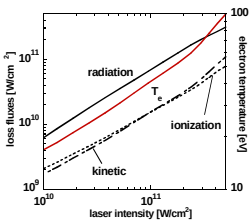

Fig. A3. Laser intensity dependence of various loss fluxes, radiation flux (black solid line), kinetic energy loss flux (dash dotted line), ionization loss flux (dotted line) and electron temperature (red) for Sn target.

The power balance model thus obtained has been applied for the prediction of CE experiments performed at Osaka. Figure A4 shows that the prediction agrees well the experiments not only the scaling law of CE, but also the absolute value of the maximum conversion efficiency 3 % [7].

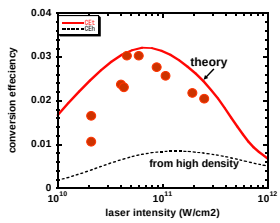

Fig. A4. Laser intensity dependence of conversion efficiency, experiments after Shimada et al. [5]: (dot) and theory after Nishihara et al. [1]: (red solid line) for Sn target with 1.2 ns laser pulse.

Appendix B. Self-Similar Solution of Fast Ion energy

A new self-similar solution has been developed which describes an expansion of a finite plasma mass into vacuum with a full account of charge separation effects [8]. Electrons are assumed to be rapidly heated to a uniform temperature and the subsequent plasma expansion is described by two charged fluids coupled via a self-consistent electric field. The maximum energy of accelerated ions are analytically calculated only from the ratio of the plasma radius to the Debye length. Since the Debye length $\lambda_D=(T_e/4\pi ne^2)^{1/2}$ is determined from the electron temperature and electron number density, the maximum energy can be controlled by changing the initial density of the heated plasma for given electron temperature and total mass as shown in Sec. IV. The analytical solutions agree well with different experimental results observed as shown in Fig. B1 [8].

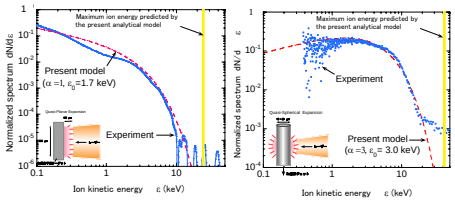

Fig. B1. Comparison of fast ion spectra between self-similar solution and experiments for planar target (left) and cylindrical target (right) after Murakami et al. [8].

References

[1] K. Nishihara *et al.,* "EUV Sources for Lithography" SPIE Press, Chap. 11 (2006)
[2] Y. Shimada et al., Appl. Phys. Lett. **86**, 051501 (2005).
[3] S. Fujioka *et al.,* Phys. Rev. Lett., **95**, 235004 (2005).
[4] T. Ando *et al.,* Appl. Phys. Lett, **89**, 151501 (2006).
[5] S. Namba *et al.*, Appl. Phys. Lett. **88**, 171503 (2006).
[6] T. Higashiguchi *et al* APL. **88**, 201503 (2006); T. Higashiguchi *et al*., SPIE **6151**, 615145 (2006).
[7] S. Fujioka *et al.*, SPIE, 6151, 61513V (2006).
[8] M. Murakami *et al*, Phys. Plasmas **13**, 012105 (2006); M. Murakami *et al*., *ibid* **12**, 062706 (2005).